ПРИБОРЫ И МЕТОДЫ ЭКСПЕРИМЕНТАЛЬНОЙ ФИЗИКИ / INSTRUMENTS AND METHODS OF EXPERIMENTAL PHYSICS

Identification of Defects in Products Made from Honeycomb Composite Materials Using Infrared Scanning Thermography

D. Yu. Golovin[a], **A. G. Divin**[a, b], **A. A. Samodurov**[a],
Yu. A. Zaharov[a, b], **A. I. Tyurin**[a], **Yu. I. Golovin**[a]✉

[a] *Derzhavin Tambov State University* (*Tambov, Russian Federation*)
[b] *Tambov State Technical University* (*Tambov, Russian Federation*)
✉ *nano@tsutmb.ru*

Abstract

Introduction. Recently, sandwich-structured composite materials based on honeycomb core and strong thin shells have become widespread.
However, these materials are characterized by manufacturing and operational flaws such as "non-gluing" and "delamination" that is the breaking of the bonds between the shell and the honeycomb core that result in the deterioration in the mechanical, acoustic and thermal properties of the material.
Aim of the Study. The study is aimed at developing effective methods for detecting flaws in gluing shell with comb core in honeycomb polymer materials.
Materials and Methods. The article describes a method for detecting these flaws using scanning thermography with a linear heat source, based on the estimation and subsequent analysis of the distribution of local temperature field gradients on the product surface.
Results. The experiments were carried out on a model polymer specimen with an embedded artificial flaw; there were shown the main sources of emerging noise, control errors, and the ways to reduce their influence; a numerical method for assessing the accuracy of the flaw measurement method was proposed.
Discussion and Conclusion. Tests carried out on a control specimen showed that the proportion of errors in measuring a defect does not exceed 12%.

Keywords: scanning thermography, non-destructive testing, composite materials, honeycomb core, flaw detection, delamination

Идентификация дефектов изделий из сотовых композиционных материалов методом инфракрасной сканирующей термографии

Д. Ю. Головин [1], **А. Г. Дивин** [1, 2], **А. А. Самодуров** [1],
Ю. А. Захаров [1, 2], **А. И. Тюрин** [1], **Ю. И. Головин** [1] ✉

[1] *Тамбовский государственный университет
имени Г. Р. Державина
(г. Тамбов, Российская Федерация)*
[2] *Тамбовский государственный технический университет
(г. Тамбов, Российская Федерация)*
✉ *nano@tsutmb.ru*

Аннотация

Введение. В последнее время получили широкое распространение сендвич-структурированные композиционные материалы на основе сотовых заполнителей в тонкой, но прочной оболочке. К сожалению, для таких материалов характерно образование производственных и эксплуатационных дефектов типа «непроклей» и «отслоение», заключающихся в нарушении связей между обшивкой и сотовым заполнителем, приводящих к ухудшению механических, акустических и тепловых свойств материала.

Цель исследования. Целью статьи является разработка эффективных методов обнаружения дефектов клеевого соединения обшивки с сотовым наполнителем сендвича.

Материалы и методы. В работе описан способ обнаружения дефектов при помощи сканирующей термографии с линейным источником тепла, основанный на вычислении и последующем анализе распределения локальных градиентов температурного поля на поверхности изделия.

Результаты исследования. Проведены эксперименты на модельном полимерном образце с заложенным искусственным дефектом, показаны основные источники возникающих шумов и ошибок контроля, способы снижения их влияния, предложен численный способ оценки точности метода определения дефекта.

Обсуждение и заключение. Проведенные на контрольном образце испытания показали, что доля ошибок при определении дефекта не превышает 12 %.

Ключевые слова: инфракрасная термография, неразрушающий контроль, композиционные материалы, сотовый заполнитель, дефектоскопия, дефект

Конфликт интересов: авторы заявляют об отсутствии конфликта интересов.

Introduction. The development of modern technology is impossible without the introduction of materials that meet the highest requirements for strength, rigidity and reliability. Such materials include composites with an internal honeycomb core and an external shell made of a polymer composite material glued to it. Honeycomb structures can be made from various types of metallic[1] [1; 2] and non-metallic materials [3], such as aluminum alloy [5–6], stainless steel [7; 8], Nomex [9; 10], craft paper [11; 12] and glass fiber [13; 14]. There are widely used honeycomb composites in which the filler (plastic polymer) is made of aramid paper impregnated with phenolic resins, resulting in the formation of a honeycomb hexagonal thin-walled structure.

Their superior physical, mechanical and other structural properties such as low density, corrosion resistance, fire resistance, good thermal insulation and high compressive strength, and good fatigue strength make aramid paper honeycomb composites the base material to make details for aerospace, automotive (race car), high-speed railway and shipbuilding industries, and for the parts of sport equipment and safety helmet. In the aircraft industry, honeycomb composites are used primarily for floors, doors, flaps, wing fairings, rudders, overhead storage compartments, ceilings, sidewall panels, engine cowlings, spoilers, nacelles and fairings.

However, in manufacturing of the products from these materials and during their operation, there may be formed such flaws as "non-gluing" and "detachment" that is the breaking of bonds between the shell and honeycomb. These flaws reduce the strength and rigidity of materials that increases the risk of destruction of the product during its operation and makes the procedure for flaw detection of these materials in demand.

Currently, ultrasonic testing is used as the main method for detecting flaws in honeycomb composites. However, the sandwich structures of these materials are characterized by rapid attenuation of ultrasonic waves with frequencies above 1 MHz, which significantly complicates the use of traditional ultrasonic methods. Therefore, new ones are being actively developed, including vibrational acoustic-ultrasonic methods operating at a frequency of less than 100 kHz, and methods based on the use of phased arrays. In addition to ultrasonic testing methods, X-ray[2], impedance methods and classical methods of free vibrations (tapping) [15] are used.

Each of these methods has its own characteristics and it is advisable to use a set of methods for the reliable flaw detection. For example, to identify subsurface flaws such as shell "detachment" or "non-gluing", it is advisable to use active scanning thermography methods, which have proven themselves to be universal, high-performance, safe, visual and easy to implement [16; 17]. These methods are based on the use of a heat source acting on the test object and further dynamic recording of the temperature field of the product surface. Anomalies in the distribution of the temperature field indicate a violation of the material structure, including the presence of the above-mentioned defects in it[3]. However, honeycomb composites, by definition, are inhomogeneous in structure

---

[1] Price T.L., Dalley G., McCullough P.C., Choquette L. Handbook: Manufacturing Advanced Composite Components for Airframes. USA: Federal Aviation Administration, Office of Aviation Research; 1997. 226 p. Available at: https://ntrl.ntis.gov/NTRL/dashboard/searchResults/titleDetail/ADA325978.xhtml (accessed 06.10.2023).

[2] ASTM E2662-15. Standard Practice for Radiographic Examination of Flat Panel Composites and Sandwich Core Materials Used in Aerospace Applications. Book of Standards Volume: 03.04. 2015 June 1. 6 p. https://doi.org/10.1520/E2662-15

[3] Golovin D.Yu., Tyurin A.I., Samodurov A.A., Divin A.G., Golovin Yu.I. [Dynamic Thermographic Methods of Non-Destructive Express Control]. Moscow: Technosphera; 2019. 214 p. (In Russ.) EDN: NATTIX

and therefore the temperature field on their surface during active thermal control is also inhomogeneous. For this reason, it is necessary to develop more complex mathematical models, methods and algorithms that make it possible to reliably identify such flaws as "non-gluing" or "detachment" using primary data obtained in the experiment.

Literature Review. The active thermography method can be applied to a greater class of materials than many other traditional quality control methods, such as radiation testing, ultrasonic testing, eddy current testing, capillary testing, etc. [18–20]. It can be applied to both metals and non-metals containing subsurface flaws such as cracks, foreign inclusions, peeling, delamination, etc.

Due to the advantage of inspecting a large area in one test, the infrared thermography is widely used for non-destructive testing of detachment flaws in honeycomb composites. Various sources of thermal excitation can be used depending on the types of flaws and types of materials. In solid polymer composite materials, the ultrasonic infrared thermography can be used [7], which makes it possible to determine the characteristics of small flaws, "closed" flaws, etc. [21]. To identify these flaws, the method of electric force thermography is also used [22]. The microwave thermography [8] has a good thermal effect on ceramic and wooden products. The eddy current thermography is used for metal products. Compared with other thermal excitation methods, the optical excitation is the simplest and most practical one. IR pulse thermography is a universal method for detecting flaws [10–12]; however, it should be taken into account that when the heat source (for example, a quartz lamp) is turned off, the inevitable effects of infrared afterglow will influence the experimental results [11].

Depending on the geometric shape of the thermal influence zone of the test object, one can distinguish:

– point-scanning, when the heating of an object is limited to a circle-shaped area of a known diameter with uniform surface rating and simultaneous moving along the object surface at a given speed and along a given trajectory [23];

– linear scanning, which is heating an object along a segment of a given length during the object movement perpendicular to this segment at a given speed [24];

– continuous heating, when a large area of the test object is exposed to heat that ensures rapid testing.

The disadvantage of continuous heating is that it is difficult to ensure uniform heating all over the surface of the test object, especially if the latter has a curved surface. Spot heating with a laser makes it possible to examine the product curved surface, but the performance of this method leaves much to be desired.

A compromise is the linear scanning method, which provides high performance and enables to examine surfaces with one-dimensional curvature. However, for honeycomb composites, the development of algorithms for identifying defective regions with shell delamination remains relevant.

Materials and Methods. For the experiments, a rectangular specimen with dimensions of $(102 \times 102 \times 12)$ mm was used. The specimen imitated a fragment of a honeycomb panel and consisted of two parts: a polymer honeycomb core and a shell glued to it. The honeycomb core was made by photopolymer 3D printing from the photopolymer Anycubic 3D Printing UV Sensitive Resin Basic produced by Shenzhen Anycubic

Technology Co., Ltd (Shenzhen, China). The 3D printer Saturn 2, manufactured by Elegoo (Shenzhen, China), was used to print. This printer is equipped with an 8K UV display, which allows printing with a horizontal resolution of 28.5 microns. Vertical resolution was 1.25 microns.

The honeycomb core is a honeycomb structure with through hexagonal cells located periodically. The dimensions of the area with cells were (100×100) mm, along the perimeter of the area with cells there was a rim of 1 mm thick. The height of the filler was 10 mm. The distance between the parallel walls of one honeycomb was 4.8 mm, the wall thickness was 0.2 mm. To simulate a delamination defect a rectangular recess with a size of (20.2×20.2) mm and a depth of 0.25 mm was made in the array of honeycomb filler cells. The indentation was built into the digital model before printing and was completed by the printer. The depth was checked using a Veeco NT 9080 profilometer and was 0.259 mm.

A fragment of fiberglass STEF GOST 12652–74 with a thickness of 0.5 mm and dimensions of (102×102) mm was used as a shell. To increase the absorption and emission coefficients of the specimen surface and prevent it from being heated in depth by radiation, its surface was painted with the matte black paint "Monarca 21200 Black" sprayed from a spray can. The thickness of the paint layer was less than 0.02 mm.

To record thermal films, there was developed an installation consisting of a three-coordinate portal-type base from a MP7 milling machine with numerical control manufactured by Purelogic (Russia, Voronezh). A heater was attached to the machine portal. At the end of the machine table, there was a support for mounting an infrared (IR) camera (hereinafter referred to as a thermal imager), which allows recording the dynamics of changes in the temperature field.

The heater was made of the Thermika 1000 W 235 V 355/272 mm SK15 reflector IR lamp placed in the reflector housing. The lamp power consumption was 1 kW. The glass bulb of the lamp had the shape of a cylinder with a diameter of 11 mm with an emitting spiral length of 272 mm. The total length of the lamp was 355 mm. The reflector housing was made of a piece of aluminum profile – a rectangular pipe measuring 40×20 mm, with a wall thickness of 1 mm, and a length of 355 mm corresponding to the overall length of the IR lamp. The housing had a 6 mm wide slot along its entire length. The housing was designed to distribute IR radiation from the lamp along the heating spot, which was a line located perpendicular to the direction of movement during scanning, provided for by the concept of active scanning thermography with a linear source.

For the installation there was used a COX CG640-G20 thermal imager manufactured by COX (South Korea, Seoul). The thermal imager used a ULIS detector – an uncooled microbolometer matrix with a resolution of (640×480) pixels. The temperature sensitivity of the detector was below 50 mK, the perceived wavelength range of IR radiation was (8...14) microns.

When recording thermal films, the specimen was placed on the installation table. The distance from the heater housing to the specimen surface was 20 mm. The portal with a fixed heater moved relative to the specimen at a speed of 20 mm/s, ensuring heating of the specimen surface to no more than 80 °C. The thermal imager remained motionless. As a result, the records of sequences of thermograms with time stamps, hereinafter referred to as "thermal films", were obtained. To work with recorded thermal films, we

used original software "Thermal Film Analyzer CRD" and several auxiliary utilities for working with data uploaded using the above application and other auxiliary functions. The developed software was written in the Processing language.

Results. For thermographic methods, the flaw is local heterogeneity of thermal physical characteristics. In the case of a honeycomb material, considering a flaw as inhomogeneity is complicated by the inhomogeneous structure of the material itself. In addition, the honeycombs have slightly different sizes and shapes, and therefore the heat removal from the heated surface layer may be uneven and irregular, and much lower than for a solid material. This is due to the fact that the entire volume of the material participates in heat removal from a solid specimen, whereas in the case of a material with a honeycomb core, heat is removed into the material mainly by thin honeycomb walls made of polymer and having low thermal conductivity. Figure 1 shows a fragment of a thermogram of a defect free region of a honeycomb composite material.
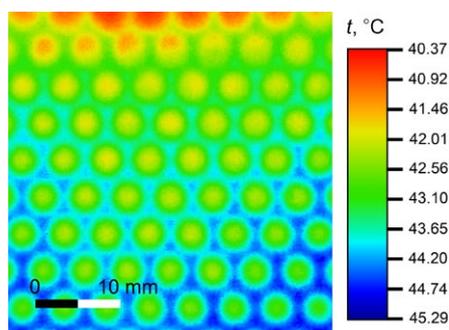

F i g. 1. Thermogram of a composite material section with honeycomb core. "Honeycombs" are clearly visible, appearing due to heat leakage along the walls of the honeycomb deep into the filler

Source: Hereinafter in this article all figures were drawn up by the authors.

During the cooling of the shell in the areas above the honeycomb walls, the temperature at the beginning of the cooling process decreased faster than above the honeycomb centers that leads to the occurrence of a thermal pattern on its surface, reflecting the structure of the honeycomb filler. After some time, the temperature equalized and the honeycombs became invisible again.

The presence of a cell wall in contact with the housing manifested itself in the occurrence of a local temperature minimum. The "detachment" flaw is characterized by poorer (or even absent) contact between the honeycomb walls and the shell. Hence, the task of detecting a flaw can be considered as the task of searching for honeycombs under the top layer of material. Thus, when a flaw became visible, the development of a numerical criterion for its detection was reduced to the problem of feature engineering. Due to heat leakage into the walls of the honeycomb, there were lateral heat flows on the surface of the material, the magnitude of which at a point corresponds to the magnitude of the gradient. Accordingly, the temperature gradient on the surface in the defect free area should be higher than in the area over delamination.

To verify this assumption, there was selected a thermal film frame immediately following after the heater output of the flaw area. Using specialized software, the gradient

values in the frame were calculated. The gradient for each point was calculated on a circular area with a radius of 6 pixels. This radius was chosen so that the gradient calculation area corresponded to the size of the area of monotonic temperature change, which made it possible to estimate the temperature gradient created by heat leakage into the nearest wall. Since the gradient was proportional to this leakage, and the amount of leakage depended on the flaw presence, the gradient can be used to determine flaw in the area of a selected point. In this case, gradients along the x and y axes were calculated as the coefficient of linear regression of temperature on the corresponding coordinate. This approach suppresses the noise, since each coefficient results from processing many pixels. Using the linear regression coefficients of temperature from x and y, the gradient magnitude and its direction (i.e., the polar coordinates of the gradient vector) were calculated. Figure 2 shows the obtained results.
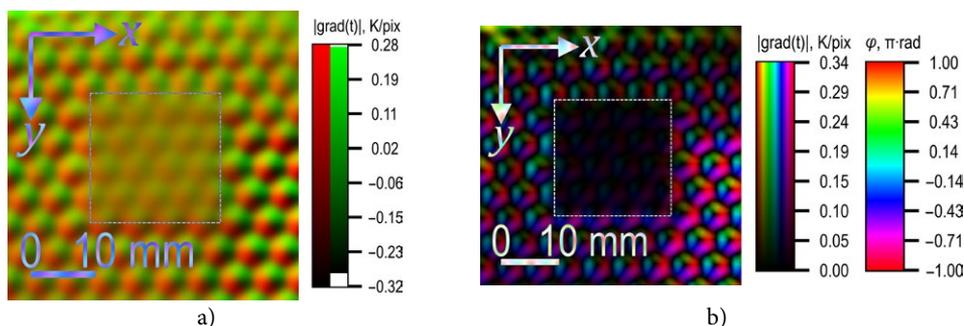

F i g. 2. Distribution of gradients in the defective area and its surroundings:
a) in rectangular coordinates, the red component is x, the green component is y; b) in polar coordinates, color saturation is the value, color tone is the direction; the defective area is shown by a dotted square

The above images clearly show that the magnitude of both the gradient components along two axes and the length of the gradient vector in the defective area were on average lower than in the defect free area. To numerically evaluate this effect on a selected fragment of a thermal film frame, a line was selected that was close to the centers of the cells (Fig. 3).
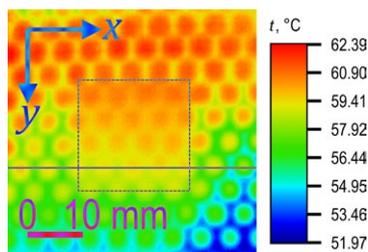

F i g. 3. Thermogram of the defective region and its surroundings.
The defective area is shown by a dotted square; the selected section is shown by a line

The gradient was calculated in a sliding window 13 pixels wide, which corresponded to the length of the section of monotonic temperature change associated with heat leakage

into the cell walls. The temperature on the line and the temperature gradient along it are shown in Figure 4.
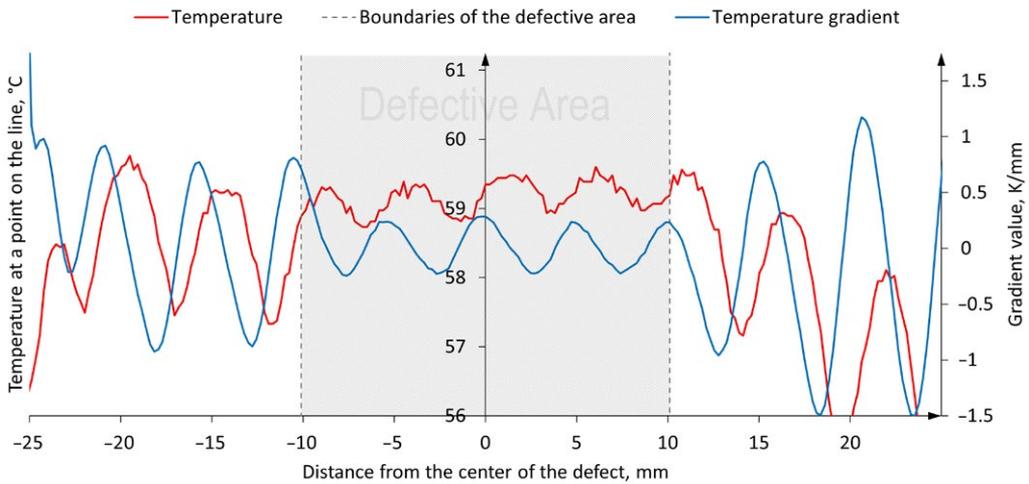

F i g. 4. Values of temperature on the selected line and temperature gradient
on the selected line along it

The average amplitude of the gradient in the defect free area was 1.91 K/mm, in the defective area it was 0.47 K/mm, which was 4.01 times lower. This amplitude discrepancy made it possible to use the temperature gradient as a criterion for flaw identification. Since the reason for the difference in gradients in the defective and defect free areas was different heat leakage into the walls of the honeycomb, the gradient should be calculated in a area that coincides in size with the value of the monotonic dependence of temperature on the coordinate. This size was the distance from the wall to the center of the cell, i.e., half the center-to-center distance of cells having a common wall. However, the value of the gradient was not constant: for points corresponding to the center of the cell or the middle of the wall, the gradient took a near-zero value, i.e., in terms of the gradient value at these points, the defective and flawless areas were indistinguishable. The discrimination problem can be solved by comparing the gradient values at points between the center and the wall, but this required an additional algorithm for searching and identifying cells. Therefore, it was advisable to introduce such an informative parameter by which one can judge the presence or absence of a flaw at each point of the observed surface, without reference to the elements of the honeycomb structure. One of the ways to do this is to use the sliding average of the absolute value of the gradient as an informative parameter for the presence or absence of a flaw at a point. As a sample implementation, a moving average of the gradient was calculated on the data shown in Figure 4 in the window which width was equal to the center-to-center distance of the cells. The distribution graph of the obtained parameter value is shown in Figure 5.
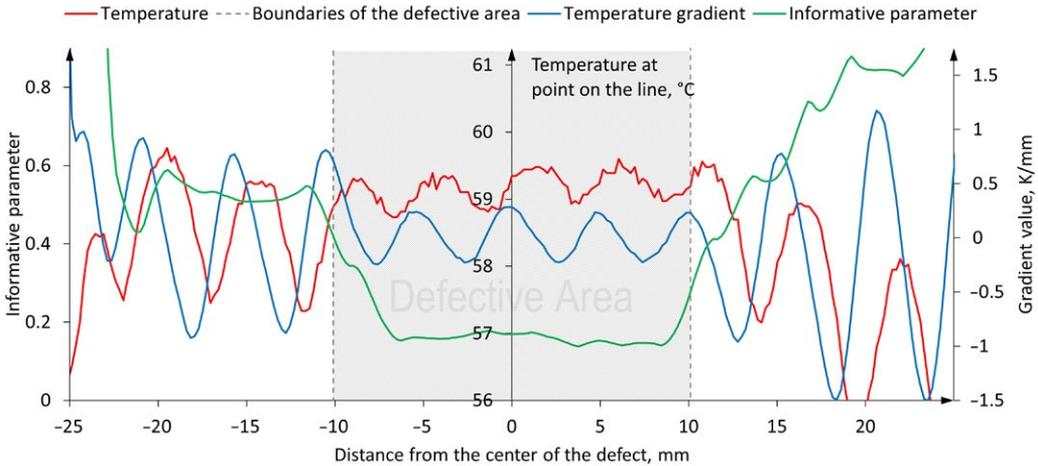
Приборы и методы экспериментальной физики

F i g. 5. Distribution of an informative parameter over a selected segment

The graph (Fig. 5) clearly shows that the selected informative parameter had a lower value in the defective area. However, the choice of a specific threshold value that would allow reliable defect detection was impossible without additional processing. Therefore, it was necessary to calculate the gradient value over a larger number of pixels and take measures to reduce the noise inherent to the method.

A way to use more pixels was the calculation of the gradient not along the section line, but around the area. However, if the gradient was not calculated on a line perpendicular to the walls, the gradient component in one direction was not sufficient. Therefore, the vector length for the neighborhood of each point was calculated. A visualization of the result is shown in Figure 6.
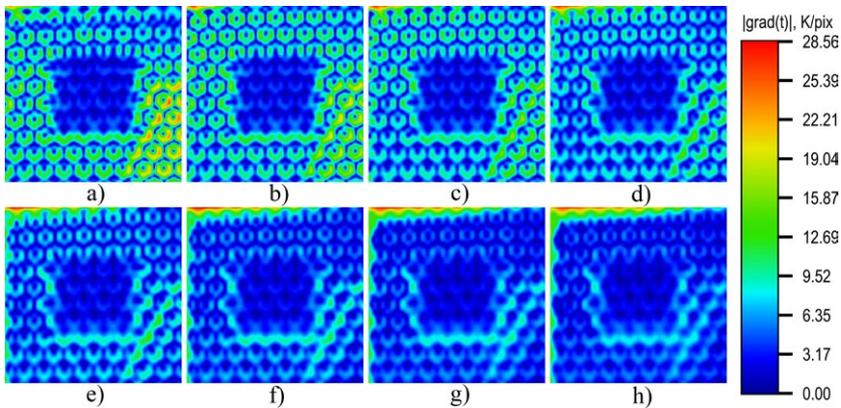

F i g. 6. Calculation of the absolute value of the gradient in the defective area and its surroundings at different times after heating: a) 0 s; b) 1 s; c) 2 s; d) 3 s; e) 4 s; f) 5 s; g) 6 s; h) 7 s

The informative parameter had a lower value in the defective area, however, developing a threshold value that allowed, without additional processing, separating the

defective and defect free areas with satisfactory accuracy was impossible, because the defective and defect free areas had too large portions of the areas in which the value of the selected informative parameter was similar. When developing a criterion, it was necessary to reduce the probability of errors of the first and second types as much as possible (Table).

T a b l e

Errors of the first and second type in defect detection

Area	Flaw found	No flaw found
Defect free	Error of the first type (α error, false positive conclusion)	Correct operation
Defective	Correct operation	Error of the second type (β error. false negative conclusion)

Source: Complited by the authors.

To reduce the likelihood of such errors, the minimum average risk criterion (Bayes criterion) was chosen. When applying the Bayes criterion, there must be some parameter indicating whether a point belongs to a defective or defect free area, a threshold value of this parameter and the area under the probability density curves of this parameter for the defective and defect free area.

To estimate the change of thermal flow in defect area the simplest informative parameter, calculated as a moving average of the absolute value of the surface temperature gradient can be used.
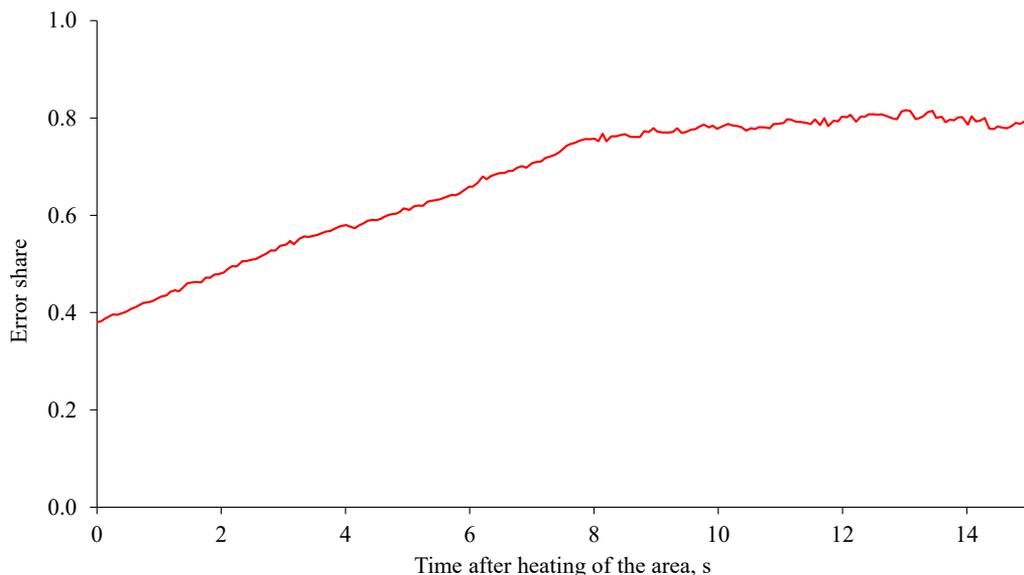

F i g. 7. Sum of Type I and Type II errors probabilities as a function of time after the passage of the heater through the section

As can be seen from the Figure 7, the minimum error value corresponded to the moment immediately after the lamp passes through and was about 38%. This value was quite large that brought the method closer in reliability to random guessing, and therefore

it was necessary to improve the method to reduce the proportion of errors. The distribution curves of the gradient value at the moment of the greatest difference (immediately after the passage of the heater) overlapped significantly (Fig. 8).
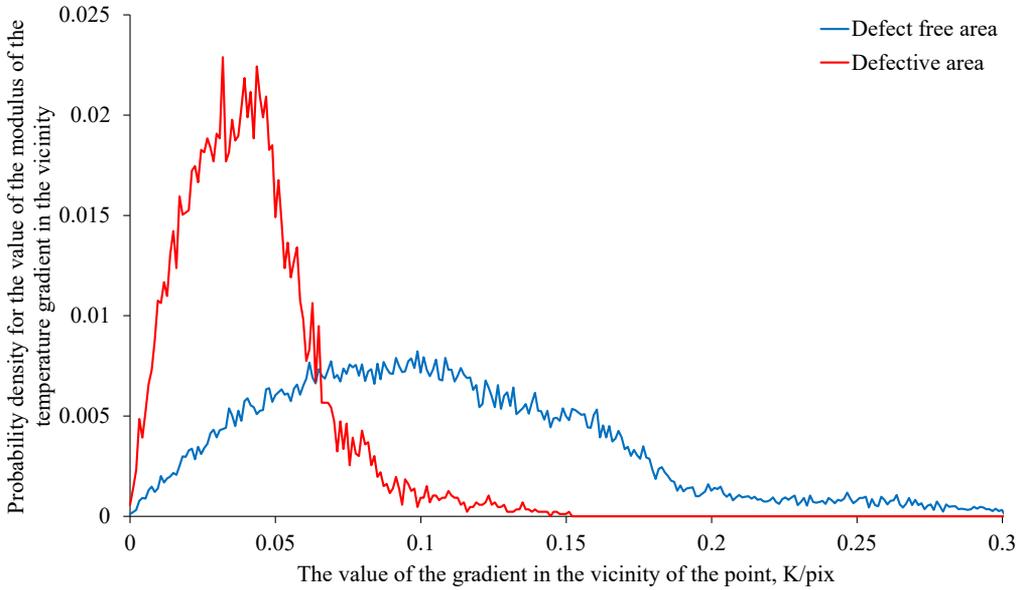

F i g. 8. Weight distribution functions of the gradient modulus

Since the pattern of spatial distribution of the gradient modulus repeats the honeycomb structure, it is proposed to use a moving average taken over a circular area, the size of which corresponds to the minimum repeating pattern of the honeycomb structure, as an informative parameter. Such averaging should lead to a decrease in parameter oscillations with a period corresponding to the cell size. The result of this transformation is shown below in Figure 9.
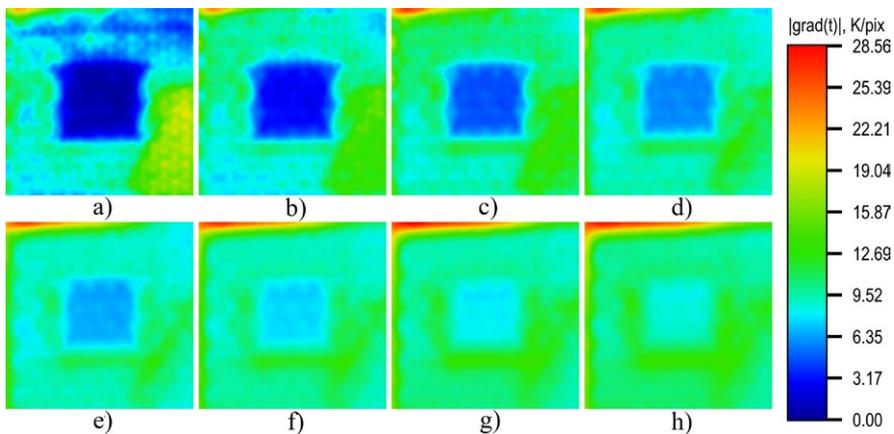

F i g. 9. For each fragment is counted from the moment of complete passage of the heater over the observed region at different times after heating: a) 0 s; b) 1 s; c) 2 s; d) 3 s; e) 4 s; f) 5 s; g) 6 s; h) 7 s

Instruments and methods of experimental physics   **275**

The change in the sum of type I and type II errors for the method is shown in Figure 10.

Averaging the result on an area improved the result significantly; the minimum error became 11.8%. The distribution of gradient modules in the defective and defect free areas at the moment of the smallest error and visualization of the gradient distribution for this moment are shown in Figure 11.
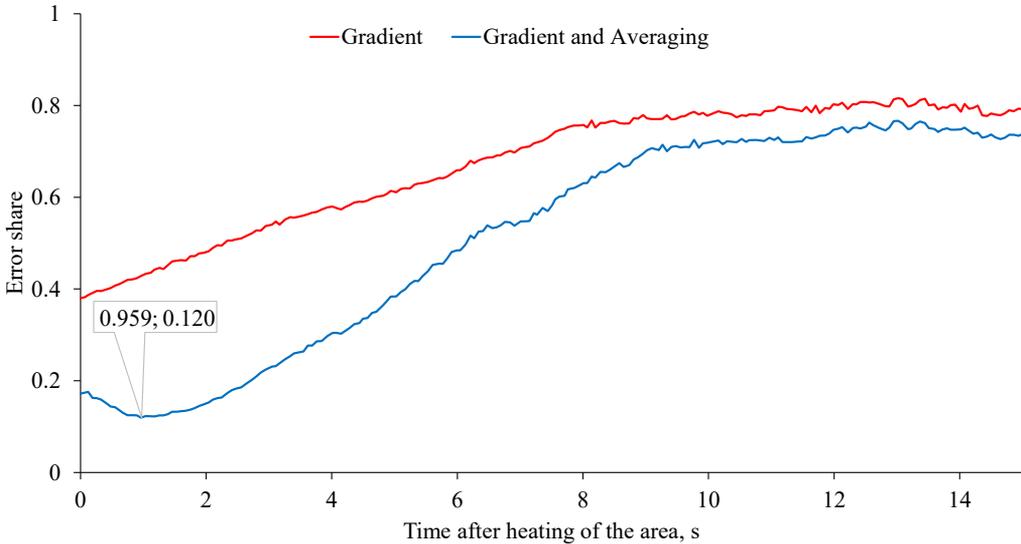

F i g. 10. Error proportion before and after improving the method by introducing averaging
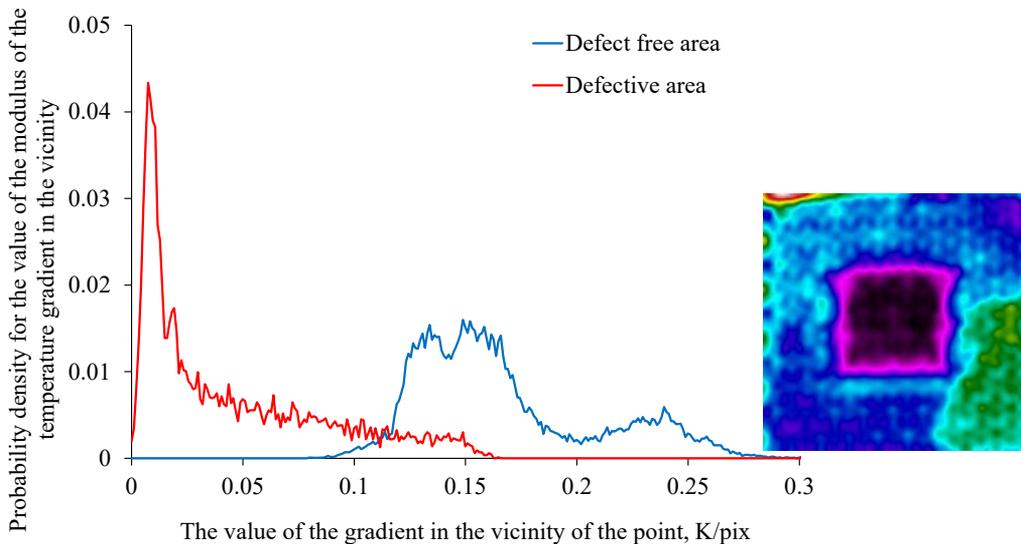

F i g. 11. Distribution of the values of the informative parameter of the improved method in the defective region and its surroundings

Discussion and Conclusion. The article discusses a method for identifying flaws in honeycomb polymer composite materials, based on calculating the gradient as an indicator that most closely corresponds to the physical meaning of the difference between heat transfer processes in defective and defect free areas. For the method, possible sources of errors were identified, and methods for compensating them were proposed. As a result of applying an improved version of the developed method, it was possible to classify defective and defect free areas with an error rate of no more than 12%. The method used traditional image processing methods applied in technical vision. This distinguishes the developed method from some of the known ones that use artificial neural networks detect and indentify defects.

The results obtained can be used to create automated systems for identifying flaws in honeycomb polymer materials.

REFERENCES

1. Ratcliffe J.G., Czabaj M.W., Jackson W.C. A Model for Simulating the Response of Aluminum Honeycomb Structure to Transverse Loading. *15th US-Japan Conference on Composite Materials Meeting* 2012;38–53. Available at: https://ntrs.nasa.gov/api/citations/20120015487/downloads/20120015487.pdf (accessed 06.10.2023).

2. Heimbs S. Virtual Testing of Sandwich Core Structures Using Dynamic Finite Element Simulations. *Computational Materials Science*. 2009;45(2):205–216. https://doi.org/10.1016/j.commatsci.2008.09.017

3. Giglio M., Manes A., Gilioli A. Investigations on Sandwich Core Properties Through an Experimental-Numerical Approach. *Composites Part B: Engineering*. 2012;43(2):361–374. https://doi.org/10.1016/j.compositesb.2011.08.016

4. Yang X., Sun Y., Yang J., Pan Q. Out-of-Plane Crashworthiness Analysis of Bio-Inspired Aluminum Honeycomb Patterned with Horseshoe Mesostructure. *Thin-Walled Structures*. 2018;125:1–11. https://doi.org/10.1016/j.tws.2018.01.014

5. Liu S., Zhang Y., Liu P. New Analytical Model for Heat Transfer Efficiency of Metallic Honeycomb Structures. *International Journal of Heat and Mass Transfer*. 2008;51(25–26):6254–6258. https://doi.org/10.1016/j.ijheatmasstransfer.2007.07.055

6. Hong S.-T., Pan J., Tyan T., Prasad P. Quasi-Static Crush Behavior of Aluminum Honeycomb Specimens under Non-Proportional Compression-Dominant Combined Loads. *International Journal of Plasticity*. 2006;22(6):1062–1088. https://doi.org/10.1016/j.ijplas.2005.07.003

7. Dharmasena K.P., Wadley H.N.G., Xue Z., Hutchinson J.W. Mechanical Response of Metallic Honeycomb Sandwich Panel Structures to High-Intensity Dynamic Loading. *International Journal of Impact Engineering*. 2008;35(9):1063–1074. https://doi.org/10.1016/j.ijimpeng.2007.06.008

8. Côté F., Deshpande V.S., Fleck N.A., Evans A.G. The Out-of-Plane Compressive Behavior of Metallic Honeycombs. *Materials Science and Engineering: A*. 2004;380(1–2):272–280. https://doi.org/10.1016/j.msea.2004.03.051

9. Rodriguez-Ramirez J.de D., Castanie B., Bouvet C. Experimental and Numerical Analysis of the Shear Nonlinear Behaviour of Nomex Honeycomb Core: Application to Insert Sizing. *Composite Structures*. 2018;193:121–139. https://doi.org/10.1016/j.compstruct.2018.03.076

10. Kim G., Sterkenburg R., Tsutsui W. Investigating the Effects of Fluid Intrusion on Nomex® Honeycomb Sandwich Structures with Carbon Fiber Facesheets. *Composite Structures*. 2018;206:535–549. https://doi.org/10.1016/j.compstruct.2018.08.054

11. Chen Z., Yan N. Investigation of Elastic Moduli of Kraft Paper Honeycomb Core Sandwich Panels. *Composites Part B: Engineering*. 2012;43(5):2107–2114. https://doi.org/10.1016/j.compositesb.2012.03.008

12. Abd Kadir N., Aminanda Y., Ibrahim M.S., Mokhtar H. Experimental Study of Low-Velocity Impact on Foam-Filled Kraft Paper Honeycomb Structure. *IOP Conference Series: Materials Science and Engineering*. 2018;290:012082. https://doi.org/10.1088/1757-899X/290/1/012082

13. Toribio M.G., Spearing S.M. Compressive Response of Notched Glass-Fiber Epoxy/Honeycomb Sandwich Panels. *Composites Part A: Applied Science and Manufacturing*. 2001;32(6):859–870. https://doi.org/10.1016/S1359-835X(00)00150-0

14. Shahdin A., Mezeix L., Bouvet C., Morlier J., Gourinat Y. Fabrication and Mechanical Testing of Glass Fiber Entangled Sandwich Beams: A Comparison with Honeycomb and Foam Sandwich Beams. *Composite Structures*. 2009;90(4):404–412. https://doi.org/10.1016/j.compstruct.2009.04.003

15. Bělský P., Kadlec M. Capability of Non-Destructive Techniques in Evaluating Damage to Composite Sandwich Structures. *International Journal of Structural Integrity*. 2019;10(3):356–370. https://doi.org/10.1108/IJSI-10-2018-0067

16. Usamentiaga R., Venegas P., Guerediaga J., Vega L., Molleda J., Bulnes F.G. Infrared Thermography for Temperature Measurement and Non-Destructive Testing. *Sensors*. 2014;14(7):12305–12348. https://doi.org/10.3390/s140712305

17. Golovin Yu.I., Golovin D.Yu., Tyurin A.I. Dynamic Thermography for Technical Diagnostics of Materials and Structures. *Russian Metallurgy (Metally)*. 2021;2021(4):512–527. https://doi.org/10.1134/S0036029521040091

18. Jiao D., Liu Z., Shi W., Xie H. Temperature Fringe Method with Phase-Shift for the 3D Shape Measurement. *Optics and Lasers in Engineering*. 2019;112:93–102. https://doi.org/10.1016/j.optlaseng.2018.09.010

19. Liu Z., Jiao D., Shi W., Xie H. Linear Laser Fast Scanning Thermography NDT for Artificial Disbond Defects in Thermal Barrier Coatings. *Optics Express*. 2017;25(25):31789–31800. https://doi.org/10.1364/OE.25.031789

20. Jiao D., Shi W., Liu Z., Xie H. Laser Multi-Mode Scanning Thermography Method for Fast Inspection of Micro-Cracks in TBCs Surface. *Journal of Nondestructive Evaluation*. 2018;37(2):30. https://doi.org/10.1007/s10921-018-0485-1

21. Kaledin V.O., Vyachkina E.A., Vyachkin E.S., Budadin O.N., Kozel'skaya S.O. Applying Ultrasonic Thermotomography and Electric-Loading Thermography for Thermal Characterization of Small-Sized Defects in Complex-Shaped Spatial Composite Structures. *Russian Journal of Nondestructive Testing*. 2020;56(1):58–69. https://doi.org/10.1134/S1061830920010052

22. Budadin O., Razin A., Aniskovich V., Kozelskaya S., Abramova E. New Approaches to Diagnostics of Quality of Structures from Polymeric Composite Materials under Force and Shock Impact Using the Analysis of Temperature Fields. *Journal of Physics: Conference Series*. 2020;1636:012022. https://doi.org/10.1088/1742-6596/1636/1/012022

23. Rellinger T., Underhill P.R., Krause T.W., Wowk D. Combining Eddy Current, Thermography and Laser Scanning to Characterize Low-Velocity Impact Damage in Aerospace Composite Sandwich Panels. *NDT and E International*. 2021;120:102421. https://doi.org/10.1016/j.ndteint.2021.102421

24. Khodayar F., Lopez F., Ibarra-Castanedo C., Maldague X. Parameter Optimization of Robotize Line Scan Thermography for CFRP Composite Inspection. *Journal of Nondestructive Evaluation*. 2018;37(1):5. https://doi.org/10.1007/s10921-017-0459-8

About the authors:

Dmitry Yu. Golovin, Cand. Sci. (Eng.), Senior Researcher at the Research Institute of Nanotechnology and Nanomaterials, Derzhavin Tambov State University (33 Internatsionalnaya St., Tambov 392000, Russian Federation), ORCID: https://orcid.org/0009-0006-8872-2121, Scopus ID: 7004150534, tarlin@yandex.ru

Alexander G. Divin, Dr.Sci. (Eng.), Professor of the Chair of Mechatronics and Technological Measurements, Tambov State Technical University (106 Sovetskaya St., Tambov 392000, Russian Federation), Senior Researcher at the Research Institute of Nanotechnology and Nanomaterials, Derzhavin Tambov State University (33 Internatsionalnaya St., Tambov 392000, Russian Federation), ORCID: https://orcid.org/0000-0001-7578-0505, Researcher ID: G-5718-2017, Scopus ID: 6506701765, agdv@yandex.ru

Alexander A. Samodurov, Cand.Sci. (Ph.-M.), Senior Researcher at the Research Institute of Nanotechnology and Nanomaterials, Derzhavin Tambov State University (33 Internatsionalnaya St., Tambov 392000, Russian Federation), ORCID: https://orcid.org/0000-0002-9600-8140, Researcher ID: P-7056-2014, Scopus ID: 6603455375, samsasha@yandex.ru

Yuriy A. Zaharov, Postgraduate Student of the Chair of Mechatronics and Technological Measurements, Tambov State Technical University (106 Sovetskaya St., Tambov 392000, Russian Federation), Junior Researcher at the Research Institute of Nanotechnology and Nanomaterials, Derzhavin Tambov State University (33 Internatsionalnaya St., Tambov 392000, Russian Federation), ORCID: https://orcid.org/0009-0002-6840-4418, sci.zah@ya.ru

Alexander I. Tyurin, Cand.Sci. (Ph.-M.), Head of the Research Institute of Nanotechnology and Nanomaterials, Derzhavin Tambov State University (33 Internatsionalnaya St., Tambov 392000, Russian Federation), ORCID: https://orcid.org/0000-0001-8020-2507, Scopus ID: 57221837737, tyurinalexander@yandex.ru

Yuriy I. Golovin, Dr.Sci. (Ph.-M.), Professor, Head of the Research Institute of Nanotechnology and Nanomaterials, Derzhavin Tambov State University (33 Internatsionalnaya St., Tambov 392000, Russian Federation), ORCID: https://orcid.org/0000-0001-6804-7057, Scopus ID: 7006092259, nano@tsutmb.ru

Authors contribution:

D. Yu. Golovin – scientific guidance, forming the structure of the article, analyzing literary data, describing the methods and technique for processing, drawing conclusions.

A. G. Divin – analyzing literary data, describing the methods and technique of processing, editing the text, drawing conclusions.

A. A. Samodurov – justification and experimental confirmation of criteria for identifying flaws.

Yu. A. Zaharov – developing the algorithms and software for recording temperature measurements using a thermal imaging camera.

A. I. Tyurin – developing measurement techniques.

Yu. I. Golovin – scientific guidance, formation of the structure of the article, analysis of literature data, writing conclusions on the work.

All authors have read and approved the final manuscript.

Об авторах:

Головин Дмитрий Юрьевич, кандидат технических наук, старший научный сотрудник НИИ «Нанотехнологии и наноматериалы» Тамбовского государственного университета имени Г. Р. Державина (392000, Российская Федерация, г. Тамбов, ул. Интернациональная, д. 33), ORCID: https://orcid.org/0009-0006-8872-2121, Scopus ID: 7004150534, tarlin@yandex.ru

Дивин Александр Георгиевич, доктор технических наук, профессор кафедры мехатроники и технологических измерений Тамбовского государственного технического университета (392000, Российская Федерация, г. Тамбов, ул. Советская, д. 106), старший научный сотрудник НИИ «Нанотехнологии и наноматериалы» Тамбовского государственного университета имени Г. Р. Державина (392000, Российская Федерация, г. Тамбов, ул. Интернациональная, д. 33), ORCID: https://orcid. org/0000-0001-7578-0505, Researcher ID: G-5718-2017, Scopus ID: 6506701765, agdv@yandex.ru

Самодуров Александр Алексеевич, кандидат физико-математических наук, старший научный сотрудник НИИ «Нанотехнологии и наноматериалы» Тамбовского государственного университета имени Г. Р. Державина (392000, Российская Федерация, г. Тамбов, ул. Интернациональная, д. 33), ORCID: https://orcid.org/0000-0002-9600-8140, Researcher ID: P-7056-2014, Scopus ID: 6603455375, samsasha@yandex.ru

Захаров Юрий Андреевич, аспирант кафедры мехатроники и технологических измерений Тамбовского государственного технического университета (392000, Российская Федерация, г. Тамбов, ул. Советская, д. 106), младший научный сотрудник НИИ «Нанотехнологии и наноматериалы» Тамбовского государственного университета имени Г. Р. Державина (392000, Российская Федерация, г. Тамбов, ул. Интернациональная, д. 33), ORCID: https://orcid.org/0009-0002-6840-4418, sci.zah@ya.ru

Тюрин Александр Иванович, кандидат физико-математических наук, директор НИИ «Нанотехнологии и наноматериалы» Тамбовского государственного университета имени Г. Р. Державина (392000, Российская Федерация, г. Тамбов, ул. Интернациональная, д. 33), ORCID: https://orcid.org/0000-0001-8020-2507, Scopus ID: 57221837737, tyurinalexander@yandex.ru

Головин Юрий Иванович, доктор физико-математических наук, директор НИИ «Нанотехнологии и наноматериалы» Тамбовского государственного университета имени Г. Р. Державина (392000, Российская Федерация, г. Тамбов, ул. Интернациональная, д. 33), ORCID: https://orcid.org/0000-0001-6804-7057, Scopus ID: 7006092259, nano@tsutmb.ru